Early-arrival waveform inversion for near-surface velocity and anisotropic parameters: inversion of synthetic data

Xukai Shen

ABSTRACT

I test different inversion parametrizations of vertical velocity and anisotropic parameter ϵ. A model space parametrized by the squares of vertical and horizontal velocity results in vertical velocity and ϵ updates with opposite signs. On the other hand, a model space parametrized by the logarithm of the vertical velocity squared and ϵ has more reasonable updates, as well as better data matching. However, ambiguity does exist in the inversion results between vertical velocity and ϵ. I clearly demonstrate these findings using a synthetic example.

INTRODUCTION

In a separate paper (Shen, 2012), I showed that in the case of early-arrival waveform inversion, changes in vertical velocity and ϵ affect data kinematics much more than δ changes do. Since δ has a minimal effect on data kinematics, I proposed joint inversion for vertical velocity and ϵ, while holding δ fixed. For such inversion, I proposed three parametrizations for joint inversion of vertical velocity and anisotropic parameter ϵ. Naive parametrization is not suitable for joint inversion, since it results in no updates to ϵ. Velocity parametrization and logarithmic slowness parametrization both seem more suitable.

In this paper, I compare the inversion results of each parametrization using two synthetic examples, one laterally invariant vertical-gradient background model with Gaussian anomalies, and one that is part of the BP 2002 velocity model with anisotropic parameters. First I will describe the equation used and the model parametrization. Then I will compare various inversion results using the two synthetic examples.

THEORY

Exact anisotropic wave equations are in the form of elastic wave equations. Acoustic anisotropic wave equations can be obtained by various approximations of the exact elastic equations. One way to do this is to set shear wave velocity to zero in the exact elastic wave equations. Detailed derivation can be found in several papers (Zhang

and Zhang, 2009; Crawley et al., 2010; Duveneck et al., 2008). The resulting acoustic anisotropic wave equations are a system of second-order equations:

$$\begin{aligned} \frac{\partial^2 p}{\partial t^2} &= {v_p}^2 (1+2\epsilon) \frac{\partial^2 p}{\partial x^2} + {v_p}^2 \sqrt{1+2\delta} \frac{\partial^2 r}{\partial z^2} \\ \frac{\partial^2 r}{\partial t^2} &= {v_p}^2 \sqrt{1+2\delta} \frac{\partial^2 p}{\partial x^2} + {v_p}^2 \frac{\partial^2 r}{\partial z^2}, \end{aligned} \tag{1}$$

where p and r are horizontal and vertical stress, respectively, v_p is vertical p-wave velocity, and ϵ and δ are anisotropic parameters (Thomsen, 1986).

The velocity parametrization defines the model space as follows:

$$\begin{aligned} m_1 &= {v_p}^2 \\ m_2 &= {v_h}^2 = {v_p}^2 (1+2\epsilon) . \end{aligned} \tag{2}$$

The logarithmic slowness parametrization defines the model space as follows:

$$\begin{aligned} m_1 &= \ln \left({v_p}^{-2} \right) \\ m_2 &= 1+2\epsilon. \end{aligned} \tag{3}$$

The non-linear conjugate gradient method is used for the inversion.

EXAMPLES

In this section, I compare the effectiveness of inversion model parametrization using two synthetic examples. In the first example, I illustrate the ambiguity between vertical velocity and ϵ, and then compare joint inversion results using the two different model parametrizations (equations 2, 3). In the second example, I compare joint inversion results using the two different parametrizations, as well as results from isotropic inversion. In both examples, I set δ to zero in both the true model and starting model, since it has very little effect on early-arrival kinematics.

Simple synthetic

The first example is relatively simple. Background velocity and ϵ are laterally invariant, and value increases with depth (Figure 1 left column). Model perturbation consists of two symmetrical Gaussian anomalies in velocity, and one Gaussian anomaly in ϵ (Figure 1 right column). The ϵ anomaly is co-located with the left velocity anomaly. The true model consists of the background model plus the model perturbation. The starting model is the background model. Recorded early-arrival data using this model consists mostly of diving waves, and the model perturbation causes non-trivial traveltime perturbation in those waves, which is the major information used for updating the starting model.

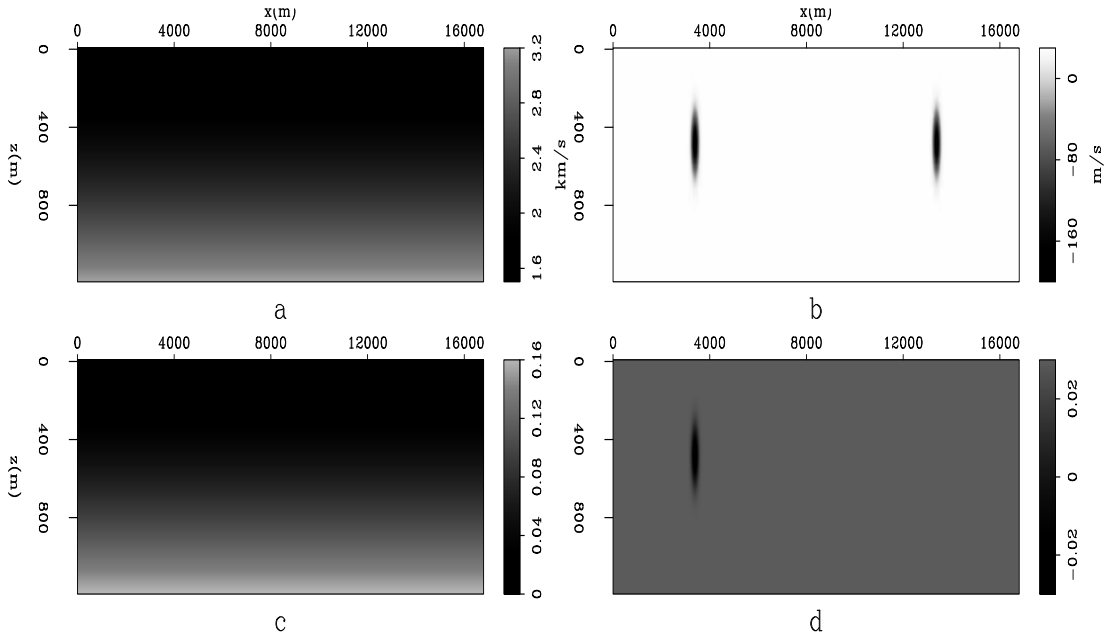

Figure 1: Background model and model perturbation. a): background velocity model; b): velocity model pertubation; c): background ϵ model; d): ϵ model pertubation. [**ER**]

This is an ideal example to illustrate the ambiguity between velocity and ϵ. I use the conventional L2 full waveform inversion (FWI) objective function (Tarantola, 1984), and vary the strength of the left velocity anomaly and the left ϵ anomaly, while setting the strength of the right velocity anomaly to zero. A total of 64 shots with 225-m spacing are modeled using the background model, with 7 Hz peak source frequency. Since the radius of all anomalies is 300 m, at a given source frequency, anomalies of this size mostly affect data traveltime rather than acting as a defractor. The traveltime differences are the major contributor to the objective function value. With receivers everywhere on the surface, the objective function value is shown in Figure 2 as a function of the two anomaly strength percentages. The valley in the center of the figure clearly indicates the ambiguity between velocity and anisotropy. If ambiguity exists even with such complete surface geometry, we can expect significant ambiguity in realistic acquisition scenarios. In such cases, proper model styling is needed in addition to data fitting.

Inversion results using velocity parametrization are shown in the left column of Figure 3. Inversion results using logarithmic slowness parametrization are shown in the right column of Figure 3. Results from using logarithmic slowness parametrization are significantly better in terms of data misfit (Figure 4). However, even with very small data misfit, inversion results are still quite different from the true model. Such results also suggest the existence of ambiguity between vertical velocity and ϵ in this simple example.

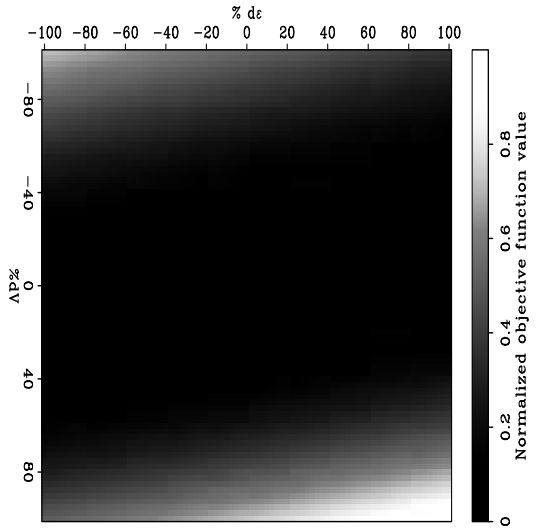

Figure 2: Normalized objective function value as a function of percentage changes in the left vertical velocity anomaly and ϵ anomaly strength. The vertical axis indicates the percent change in the vertical velocity anomaly. The horizontal axis indicates the percent change in the ϵ anomaly. [**NR**]

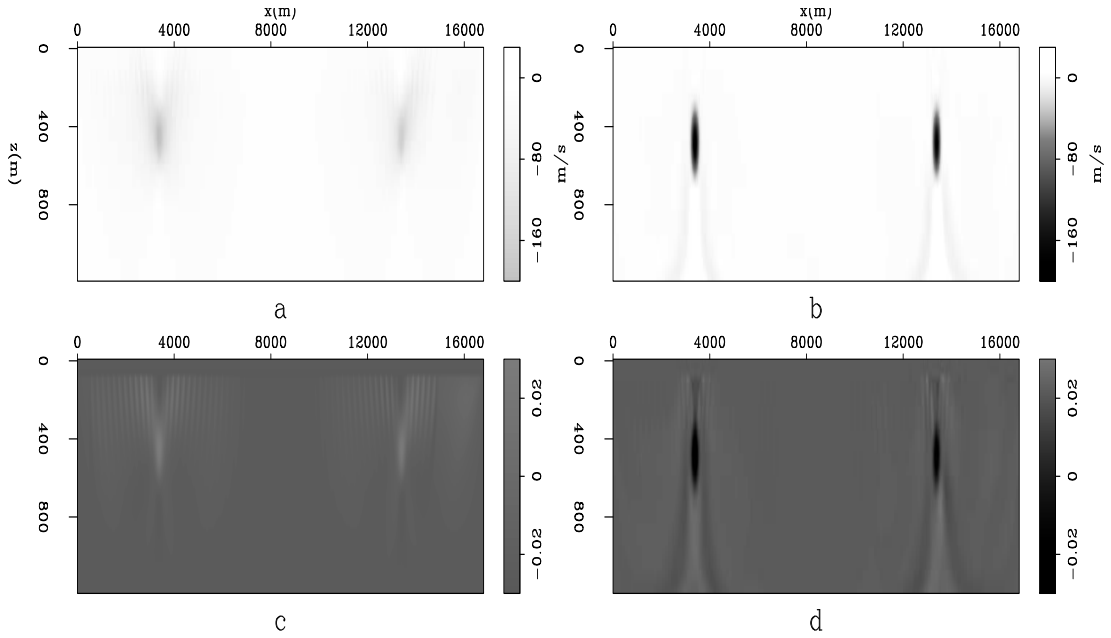

Figure 3: Inverted model perturbation. a): expressed in vertical velocity using velocity parametrization; b): expressed in vertical velocity using logarithmic slowness parametrization; c): expressed in ϵ using velocity parametrization; d): expressed in ϵ using logarithmic slowness parametrization. [**CR**]

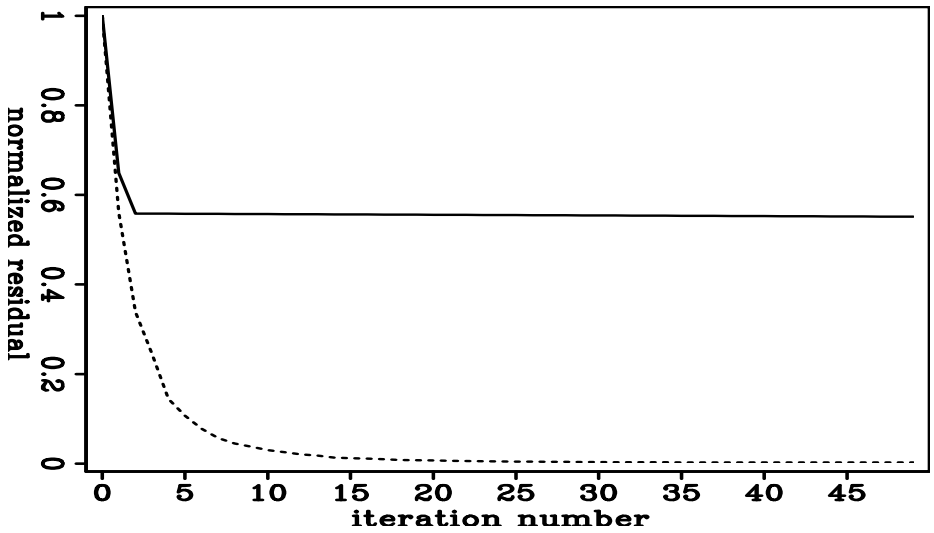

Figure 4: Data residual as a function of iteration number during inversion using different inversion model parametrization. Continuous: velocity parametrization; dashed: logarithmic slowness parametrization. [**CR**]

Complex synthetic

In this example, I invert the synthetic model shown in Figure 5. For joint inversion, starting models of vertical velocity and ϵ are a smoothed version of the true models without the shallow gas-pockets (Figure 6), and the δ parameter is fixed at zero. A total of 64 shots with 320-m shot spacing are used, with sources of 7 Hz peak frequency. The gas pocket sizes range from several hundred meters to almost two thousand meters. Given the dominant wavelength of the source wavelet, gas pocket sizes are on the order of several wavelengths, ensuring that most of the data misfit comes from the diving-wave traveltime difference. For simplicity, we assume that receivers are everywhere on the sea surface. The true model produces both refraction and reflection data. However, data masks are used during inversion to make sure that the inversion relies only on matching early arrivals that precede direct arrivals. Joint inversion results are shown for velocity parametrization in Figure 7, and for the logarithmic slowness parametrization in Figure 8. The logarithmic slowness parametrization yields a far superior model compared to inversion using velocity parametrization. This can also be seen in the data misfit comparison (Figure 9).

For velocity parametrization, the gradient for vertical velocity has more terms than the gradient for horizontal velocity. This leads to more updates for vertical velocity than for horizontal velocity and tends to result in the epsilon update having a sign opposite to that of the vertical velocity update. Since this is not always geologically true, such inversion model parametrization is not ideal, at least for gradient-based inversion methods. Inversion using logarithmic slowness parametrization results in reasonable data matching; however, relatively smooth ϵ updates in the inversion result do suggest data misfit from ambiguity between ϵ changes and vertical velocity changes.

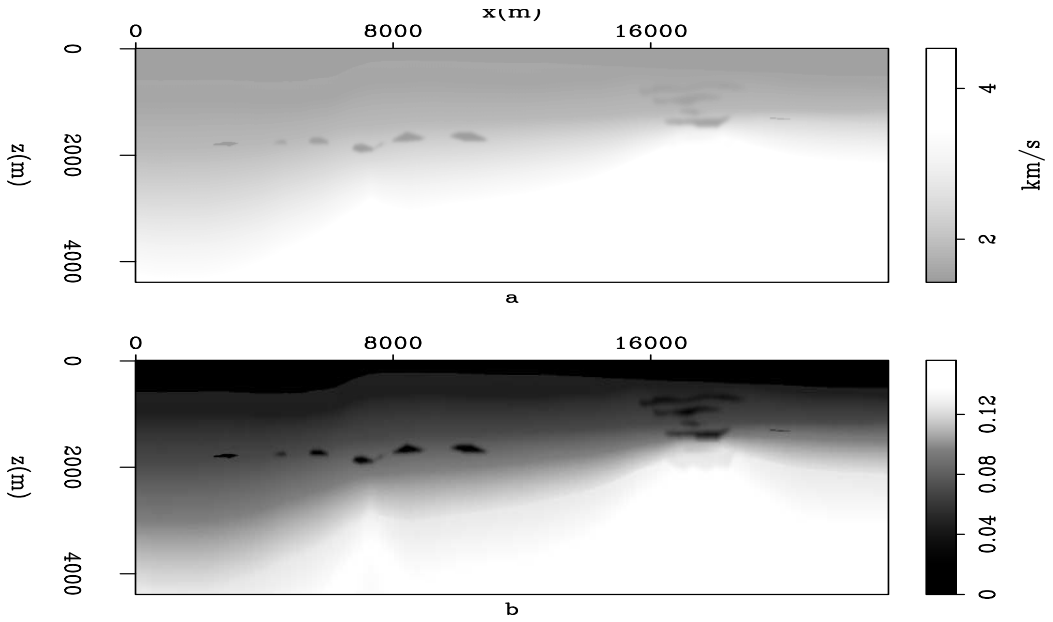

Figure 5: True model. a): velocity model; b): ϵ model. [**ER**]

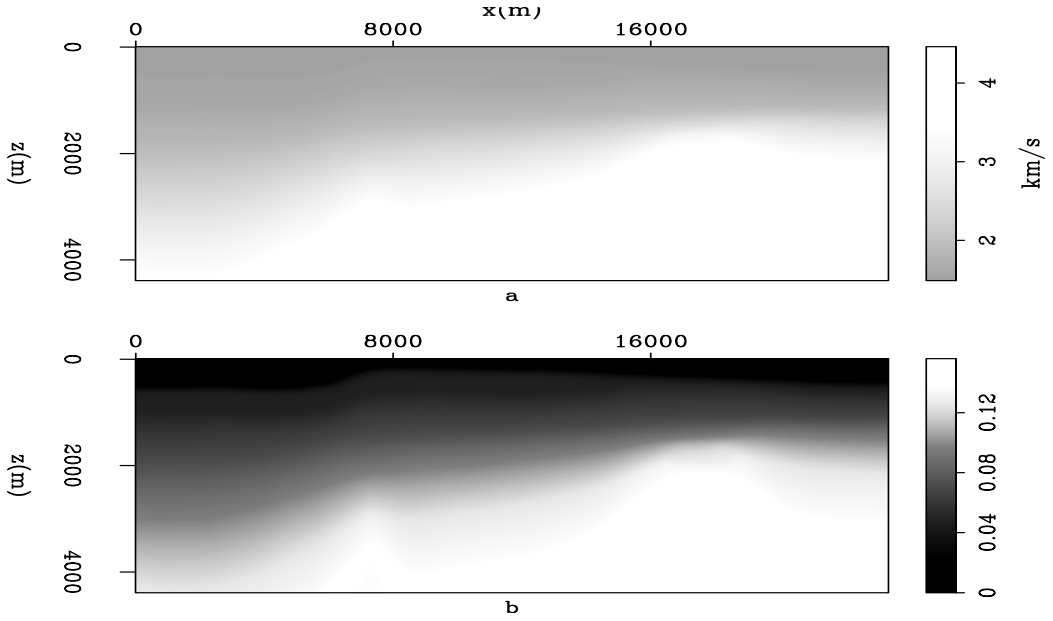

Figure 6: Starting model. a): velocity model; b): ϵ model. [**ER**]

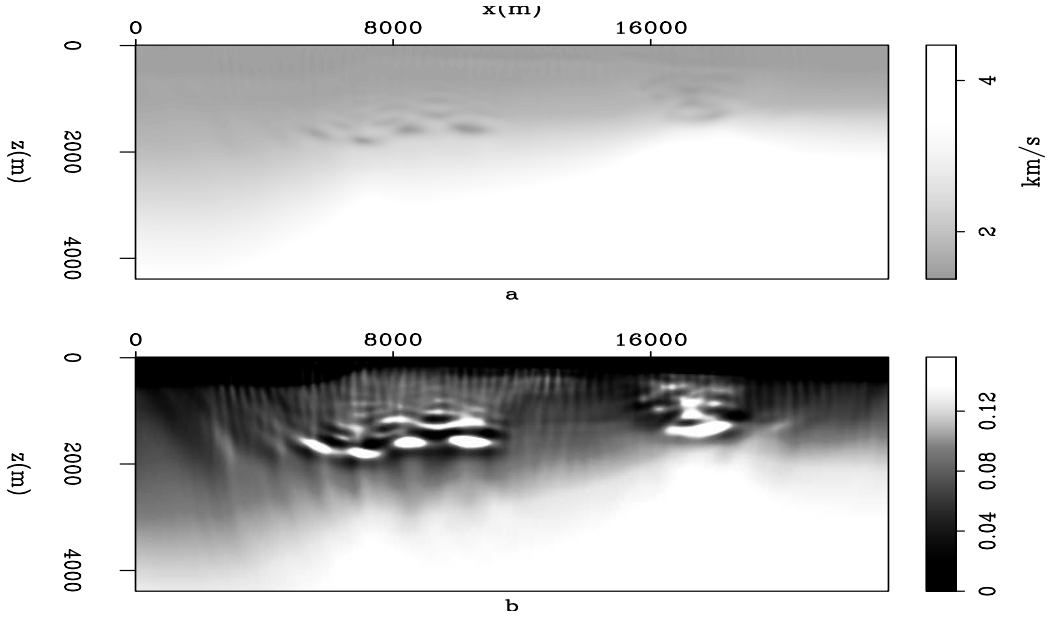

Figure 7: Inversion results using velocity parametrization, expressed in vertical velocity and ϵ. a): velocity model; b): ϵ model. [**CR**]

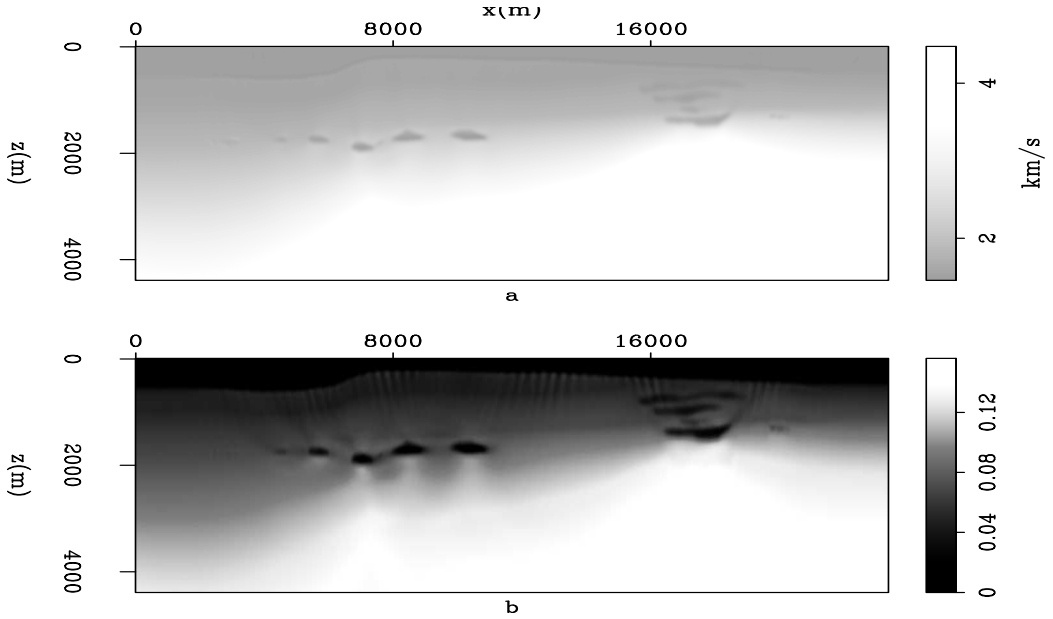

Figure 8: Inversion results using logarithmic slowness parametrization, expressed in vertical velocity and ϵ. a): velocity model; b): ϵ model. [**CR**]

This ambiguity can potentially be mitigated by proper model styling.

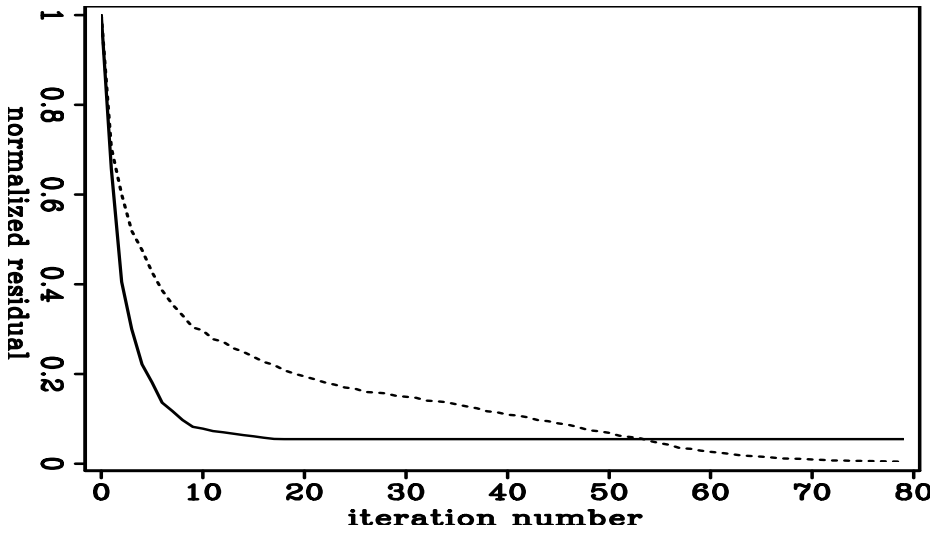

Figure 9: Data residual as a function of iteration number during inversion using different inversion model parametrizations. Continuous: velocity parametrization; dashed: logarithmic slowness parametrization. [**CR**]

For comparison, isotropic inversion is also performed on this model. Two types of starting velocity are used: one is the same vertical velocity model as the starting model in joint inversion, and the other is the horizontal velocity model calculated from the vertical velocity and ϵ of the starting model used in joint inversion. The inversion results and data misfit are shown in Figures 11 and 12. It is obvious that inversion results are more geologically reasonable starting from the smooth vertical velocity model. This is also supported by data misfit. Comparing results with the true vertical velocity model and the true horizontal velocity model (Figure 10), it is interesting to see that in the better inversion result, the shallow parts mostly agree with the true vertical velocity model, and the deeper parts mostly agree with the true horizontal velocity model.

CONCLUSIONS

I compared inversion results using different model-space parametrizations for early-arrival waveform inversion. Results from isotropic inversion of anisotropic data are similar to the vertical velocity in the shallow parts of the model, and closer to the horizontal velocity model in the deeper part. For joint inversion of vertical velocity and the ϵ parameter, I kept δ fixed due to the insensitivity of the data to δ changes. A model space parametrized by squares of vertical velocity and horizontal velocity tends to produce updates in vertical velocity and ϵ that have opposite signs, which is unfavorable in practical inversion. The model space parametrized by the logarithm of the squared vertical slowness and epsilon has more reasonable updates and gives

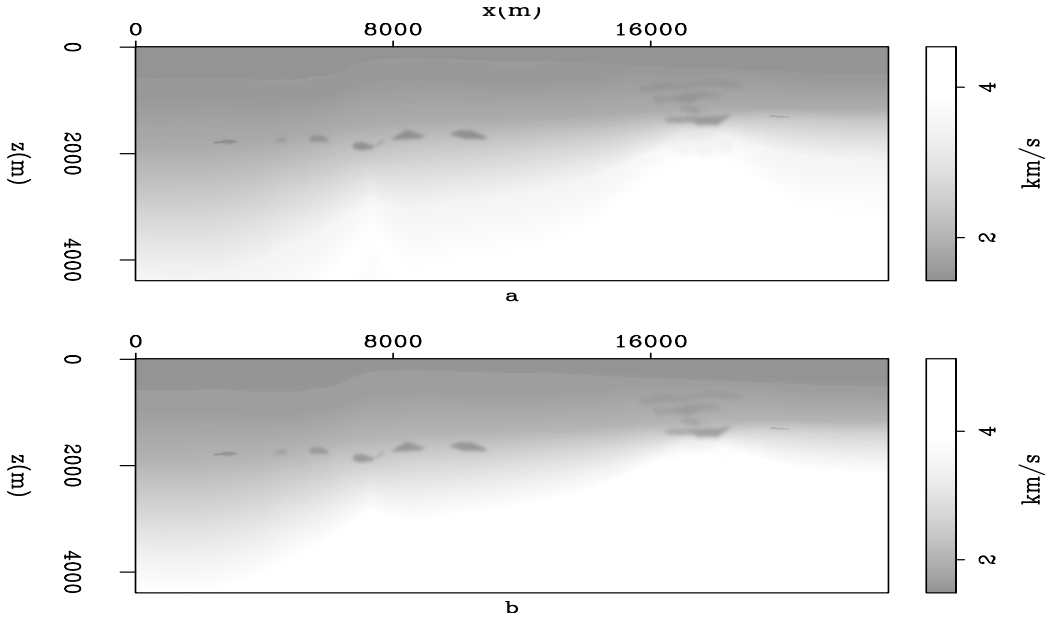

Figure 10: True velocity model. a): vertical velocity; b): horizontal velocity. [**CR**]

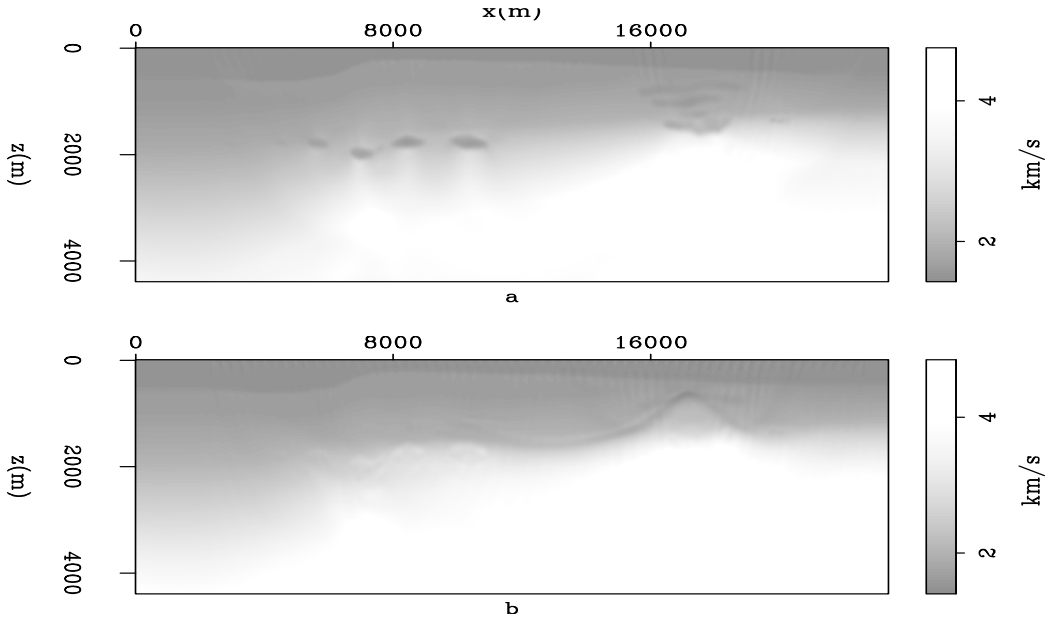

Figure 11: Velocity model from isotropic inversion starting from, a): smooth vertical velocity; b): smooth horizontal velocity. [**CR**]

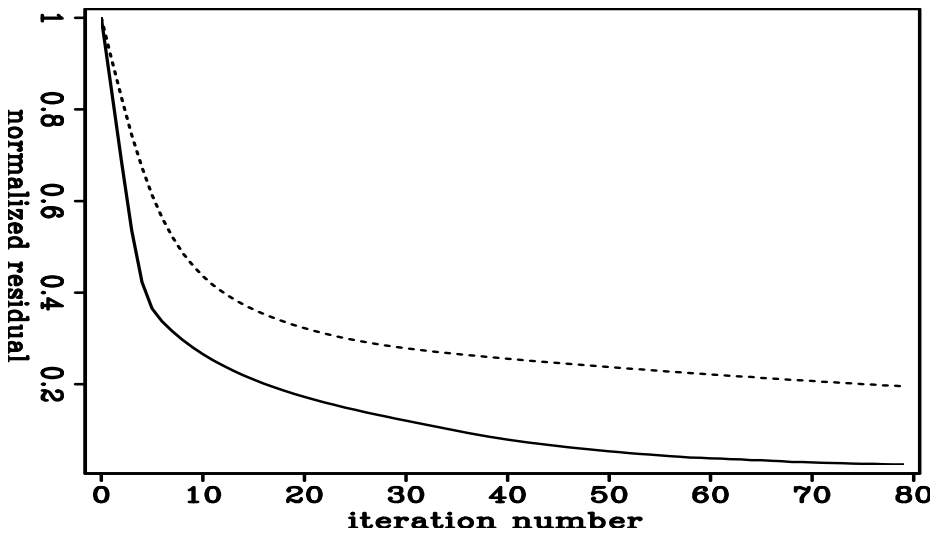

Figure 12: Data residual as a function of iteration during isotropic inversion using different starting models. Continuous: starting from smooth vertical velocity; dashed: starting from smooth horizontal velocity. [**CR**]

far better inversion results. However, ambiguity does exist in the inversion results between vertical velocity and ϵ. The same data misfit can be explained by different combinations of vertical velocity and ϵ, so proper model styling is needed to reduce such ambiguity.

REFERENCES

Crawley, S., S. Brandsberg-Dahl, J. McClean, and N. Chemingui, 2010, TTI reverse time migration using the pseudo-analytic method: The Leading Edge, **29**, 1378.

Duveneck, E., P. Milcik, P. M. Bakker, and C. Perkins, 2008, Acoustic VTI wave equations and their application for anisotropic reverse-time migration: SEG Expanded Abstracts, 2186–2189.

Shen, X., 2012, Early-arrival waveform inversion for near-surface velocity and anisotropic parameters: Modeling and sensitivity kernel analysis: SEP-Report, **147**, 73–82.

Tarantola, A., 1984, Inversion of seismic reflection data in the acoustic approximation: Geophysics, **49**, 1259–1266.

Thomsen, L. A., 1986, Weak elastic anisotropy: Geophysics, **51**, 1954–1966.

Zhang, Y. and H. Zhang, 2009, A stable TTI reverse time migration and its implementation: SEG Expanded Abstracts, 2794–2797.